


Indefinite temporal order without gravityKacper Dębski ^{1,*}, Magdalena Zych,^{2,3,†} Fabio Costa,^{3,4,‡} and Andrzej Dragan^{1,5,§}¹*Institute of Theoretical Physics, University of Warsaw, Pasteura 5, 02-093 Warsaw, Poland*²*Department of Physics, Stockholm University, Roslagstullsbacken 21, 106 91 Stockholm, Sweden*³*Australian Research Council Centre for Engineered Quantum Systems, School of Mathematics and Physics, The University of Queensland, St Lucia, QLD 4072, Australia*⁴*Nordita, Stockholm University and KTH Royal Institute of Technology, Hannes Alfvéns väg Stockholm, 106 91, Sweden*⁵*Centre for Quantum Technologies, National University of Singapore, 3 Science Drive 2, 117543 Singapore, Singapore*

(Received 18 January 2023; revised 18 July 2023; accepted 23 October 2023; published 5 December 2023)

According to the general theory of relativity, time can flow at different rates depending on the configuration of massive objects, affecting the temporal order of events. Combined with quantum theory, this gravitational effect can result in events with an indefinite temporal order when a massive object is prepared in a suitable quantum state. This was argued to lead to a theory-independent test of the nonclassical order of events through the violation of Bell-type inequalities for temporal order. Here we show that the theory independence of this protocol is problematic: one of the auxiliary assumptions in the above approach turns out to be essential, while it is explicitly theory dependent. To illustrate this problem, we construct a complete scenario where accelerating particles interacting with optical cavities result in a violation of temporal Bell inequalities. Due to the equivalence principle, the same problem arises when one considers the gravitational case, and thus theory-dependent additional assumptions are needed behind Bell inequalities for temporal order to interpret a violation of the final inequalities as a signature of indefinite temporal order.

DOI: [10.1103/PhysRevA.108.062204](https://doi.org/10.1103/PhysRevA.108.062204)**I. INTRODUCTION**

Quantum theory and general relativity rest on very different foundations. In quantum theory, systems, in general, do not possess definite physical properties prior to their measurement; however, processes take place on a fixed background space-time, where the causal relations between events—spacelike or timelike—are defined independently of any operation or physical process. On the other hand, in general relativity, causal relations are not fixed *a priori*, as the geometry depends on the configuration of mass-energy. Therefore, it is expected that a unification of the two theories should result in nonclassical, or indefinite, causal structure [1,2].

However, the physical meaning of such an indefinite causal structure is not clear. An early example of an indefinite causal structure was provided by the so-called quantum switch, introduced in Ref. [3], where it was shown that quantum degrees of freedom (DoFs) controlling the order of operations can generate evolution that cannot be described in terms of a standard quantum circuit. Most approaches to quantum gravity attempt to establish a complete theoretical framework (that would include, among other features, description of nonclassical space-times and how they arise) [4,5] but do not offer

a direct physical interpretation of such non-classical causal structure.

Recent work has proposed a Gedanken experiment to directly pinpoint the physical meaning of the nonclassicality of temporal order, independently of the details of a full quantum theory of gravity [6]. The idea is that a superposition of mass configurations will induce a corresponding nonclassical time dilation on any system one might use as a “clock” to identify space-time events, effectively producing, for example, a superposition of different orderings of timelike events. It was argued that, following a specific protocol, one can perform a task—the violation of a Bell inequality—that would be impossible if the temporal order of events was classical. The protocol was argued to provide a theory-independent certification of the nonclassicality of temporal order among a set of events.

Here we present an in-principle complete scheme where accelerating particles interact with quantum fields according to their own internal clock DoFs. Such a purely special-relativistic setting avoids any need for assuming physics beyond a currently tested regime, especially, the back-action on space-time of the involved matter is negligible. A superposition of the clock states of motion causes the corresponding nonclassical time dilation, as investigated in Ref. [7]. By letting the particles evolve in superposition along such accelerating trajectories, we show that the particle-field interaction events reproduce the “entanglement of temporal order” found in the gravitational case [6]. Remarkably, our study reveals that a violation of the Bell inequalities persists even when the entangled events are spacelike, challenging the interpretation

*kdebski@fuw.edu.pl

†magdalena.zych@fysik.su.se

‡fabio.costa@su.se

§dragan@fuw.edu.pl

that the protocol uniquely identifies nonclassical temporal order of necessarily timelike events. We find that this is due to the failure of one of the auxiliary assumptions made in Ref. [6], namely, that the superposed amplitudes only differ in the event order, while all local evolutions are trivial, including the free evolution of the systems which are measured to reveal the violation of Bell inequalities. We also argue that the failure of this assumption is ubiquitous and would be present in a generic dynamical context, including a gravitational implementation of the protocol. We also propose an interpretation of the Bell inequality violation in scenarios where nonclassicality of temporal order cannot possibly explain the results (e.g., for spacelike separated events mentioned above).

Our results raise a fundamental question, whether it is possible to formulate an operational scenario that can unambiguously discriminate the nonclassicality of the causal structure of space-time from dynamical effects, necessarily present in its physical implementations, or other laboratory implementations of quantum causal structures [8–14]. We present a discussion on what extensions to the original protocol might be required in order to achieve that.

Furthermore, a flat space-time version of the protocol may allow for a laboratory implementation as well as provide further insights into the requirements entering the original, gravitational, argument. Finally, it seems probable that the quantum indeterminacy of space-time structures lies at the heart of the still unknown quantum theory of gravity [15,16], therefore comparing special relativistic and gravitational schemes could also provide insights into possible violations of the equivalence principle due to quantum effects.

Throughout this paper, we use natural units, for which we have $\hbar = c = 1$.

A. Gravitational implementation of an indefinite temporal order

For later reference, we will briefly review the salient aspects of the protocol introduced in Ref. [6]. The goal of the protocol is to realize four events, A_1, B_1, A_2, B_2 , whose pairwise order is entangled: A_1 is in the causal past-past lightcone of B_1 , denoted $A_1 < B_1$ when $A_2 < B_2$, and A_1 is in the causal future-future lightcone of B_1 , denoted $A_1 > B_1$ when $A_2 > B_2$, (or an exemplary depiction of two events A and B being in the relation $A < B$ or $A > B$ —see Fig. 1. The full scenario is arranged such that this entanglement leads to correlations that do not admit a local classical explanation, which is formalised in analogy to Bell-like scenarios for local classical properties. Crucially, an “event” is here understood operationally as something that happens at a particular time and place and thus is defined by some physical reference system. Likewise, for a fixed event A , the relation $A < B$ operationally defines as future such events B that are reachable by a photon or a massive particle sent at event A .

In the considered protocol, the reference systems are four clocks, a_1, b_1, a_2, b_2 , while the events are associated with quantum operations performed on some additional system when the corresponding clock reaches a specified proper time: A_1 takes place (an operation is performed) when a_1 reaches time τ^* , B_1 takes place when b_1 reaches time τ^* , and so on.

In flat space-time, if the clocks are initially synchronized (in an arbitrary chosen reference frame), all events are

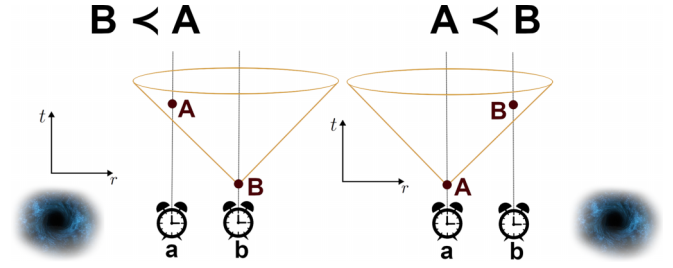


FIG. 1. Position of a mass as a control of time order. Two identical clocks a, b are synchronized (with any source mass sufficiently far away). Events A, B are defined as the location and fixed proper time τ^* of the corresponding clock. In the absence of any source mass, events A, B are spacelike. However, if a massive object is initially (just after synchronization) placed closer to clock a than to b , event A can be in the future lightcone of B (for sufficiently large τ^*), denoted $B < A$. Analogously, for the mass closer to b , event A can be up in the past lightcone of B , $A < B$.

spacelike separated. However, introducing a massive body closer to some clocks than others causes a differential time dilation, which can push some events into the future lightcone of other events. Thereby, the position of the mass provides a control of the time order of events, see Fig. 1. If the control mass is prepared in a semiclassical configuration denoted K_A , event $A_j, j = 1, 2$ is in the past of B_j , while for a different configuration, K_B , event B_j is in the past of A_j . Thus, A_j is timelike from B_j , for each mass configuration, but their order is interchanged. Moreover, for both mass configurations, the pair A_1, B_1 is spacelike from A_2, B_2 .

The full protocol also features two of the above-mentioned additional systems on which the operations are performed, S_1 and S_2 , referred to as targets. The operations at events A_1 and B_1 are applied only on the target system S_1 , while those at A_2 and B_2 are applied only on S_2 . The two target systems are initially in a product state, $|\psi\rangle^{S_1}|\psi\rangle^{S_2}$, and the considered operations are unitaries: \hat{U}^{A_1} is applied on S_1 at event A_1 , etc. Operations applied to the target system S_1 and S_2 will be referred to as wings 1 and 2, respectively, of the experiment. Then, by preparing the control mass in a superposition state, $|K\rangle = \frac{1}{\sqrt{2}}(|K_A\rangle + |K_B\rangle)$, one obtains the final state

$$|\Psi^{\text{fin}}\rangle = \frac{1}{\sqrt{2}}(|K_A\rangle\hat{U}^{B_1}\hat{U}^{A_1}|\psi\rangle^{S_1}\hat{U}^{B_2}\hat{U}^{A_2}|\psi\rangle^{S_2} + |K_B\rangle\hat{U}^{A_1}\hat{U}^{B_1}|\psi\rangle^{S_1}\hat{U}^{A_2}\hat{U}^{B_2}|\psi\rangle^{S_2}). \quad (1)$$

Next, the control mass is measured in the basis $|\pm\rangle = \frac{1}{\sqrt{2}}(|K_A\rangle \pm |K_B\rangle)$, leaving the target system in

$$|\Psi^{\text{post}}\rangle = \frac{1}{\sqrt{2}}(|\psi_A\rangle^{S_1}|\psi_A\rangle^{S_2} \pm |\psi_B\rangle^{S_1}|\psi_B\rangle^{S_2}), \quad (2)$$

where $|\psi_A\rangle = \hat{U}^B\hat{U}^A|\psi\rangle$, $|\psi_B\rangle = \hat{U}^A\hat{U}^B|\psi\rangle$, and we are using the same unitaries in the two wings, i.e., for A_1 and A_2 we have $\hat{U}^{A_1} = \hat{U}^{A_2} \equiv \hat{U}^A$, and for B_1 and B_2 we have $\hat{U}^{B_1} = \hat{U}^{B_2} \equiv \hat{U}^B$.

In general, $|\Psi^{\text{post}}\rangle$ is an entangled state, unless $|\psi_A\rangle = |\psi_B\rangle$ (and it is elementary to find examples of unitaries \hat{U}^A, \hat{U}^B such that this is not the case). In the final step of the protocol, the

TABLE I. Assumptions of Bell's theorem for temporal order (see Ref. [6]).

Assumption	Explanation
Local state	The initial state of the whole system is separable.
Local operations	All transformations performed on the systems are local .
Classical order	The events at which operations (transformations and measurements) are performed are classically ordered.
Spacelike separation	Events (A_1, B_1) are spacelike separated from events (A_2, B_2) . Additionally, the measurement of a control mass is space-like separated from both wings.
Free choice	The measurement choices in the Bell measurement are independent of the rest of the experiment.

entangled state is measured in appropriate bases that lead to a violation of a Bell inequality.

The argument presented in Ref. [6] is that, given the initial product state of the target systems, local operations that are performed in a definite order would not be able to produce entanglement, even after conditioning on the control system. Therefore, if a set of conditions is satisfied, a violation of Bell inequalities implies that the operations were not performed in a definite order (for more details, see Table I).

Another auxiliary assumption introduced in Ref. [6], which ends up as a focal point of the present paper, is that any additional evolution of the target systems (including their free evolution) between the events of interest can be neglected. In the present paper, we examine the consequences of this additional assumption. We construct a scenario in which neglecting the free part of evolution of the target is not possible. We then argue that this is a generic feature and that finding exceptions where the assumption holds requires theory-dependent analysis. For completeness of the discussion, we start by presenting a scenario that can generate a violation of Bell inequalities and then discuss the possibility of verifying the existence of indefinite temporal order solely due to the violation of these inequalities.

In Sec. IV, we focus on reproducing the gravitational protocol using special relativistic time dilation. We present an operational setting where the dynamics of all the relevant DoFs are incorporated, in particular, the DoFs whose interactions realize the four unitaries \hat{U}^A, \hat{U}^B . In Sec. IV D, we discuss our main result—that entanglement can be generated and Bell inequality for temporal order can be violated even if temporal order is classically defined—and argue that it is due to the failure of the additional assumption mentioned above, that target systems have trivial evolution apart from the unitaries marking the four space-time events of interest. In Sec. IV E, we provide the simplified example showing the importance of the free evolution. In Sec. V, we discuss the implications of our result, including the fundamental question of how to isolate quantum features of a causal structure from other nonclassical effects.

II. GENERAL SETUP

Instead of using a massive object to control the space-time geometry—and thus temporal order via gravitational time dilation—here we want to control the trajectories of particles so as to induce special-relativistic time dilation. For clarity of this scheme, we decided to provide a simple comparison between our approach and the original one presented in Ref. [6] in the form of Table II. The protocol involves several

DoFs, which can be best thought of as multiple particles glued together (up to the moment when we need to break them apart, as detailed later). We will refer to a bunch of joined particles as a molecule, although the details of what binds the particles together are irrelevant to the discussion.

Our protocol involves four molecules going through two optical cavities (two molecules per cavity). In further consideration, we will refer to everything that happens to these two cavities as two wings of the protocol because they will play the same role as the wings described in the previous section. Moreover, each molecule is composed of three particles: a clock, a detector, and a control. Figure 2 presents a general scheme of our protocol.

The clock is simply a particle with some time-evolving internal state; if the molecule evolves along a classical trajectory, the internal state evolves at a rate proportional to the trajectory's proper time. The role of the clock is to trigger an interaction between the detector and the cavity at the desired proper time. Thanks to the universality of time dilation, the protocol does not depend on the particular mechanism by which the clocks evolve—all we need is that the clock reaches

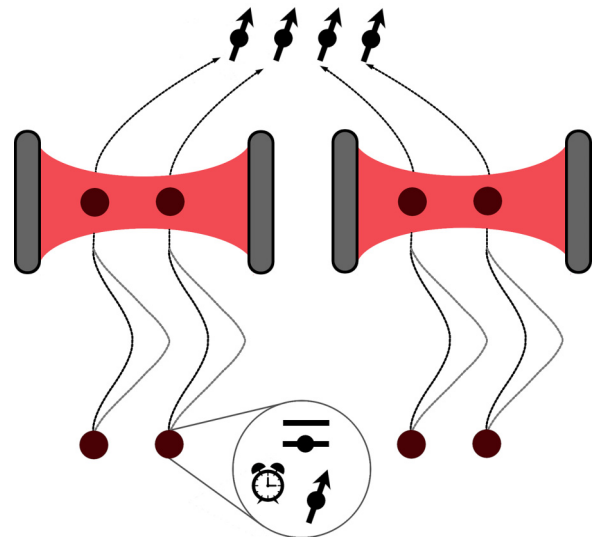


FIG. 2. General scheme of our protocol for a violation of Bell inequalities for temporal order. In each wing of the experiment, we have a quantum field in a cavity, and two composite molecules. After following entangled pairs of trajectories, the molecules interact with the fields at a fixed proper time of their internal clocks. Due to time dilation, entangled state of motion gets transferred to the order of the interaction events (as well as to other degrees of freedom of the molecules and the cavities).

TABLE II. Comparison between the degrees of freedom involved in the gravitational scheme and ours. Here we only consider the main scheme from Ref. [6] (variations of the scheme involve multiple control systems or different target DoFs.)

	Gravity	Cavity
Control system	Massive body	Spin- $\frac{1}{2}$ particles (one per molecule, two in each wing)
Target system	A single two-level system (e.g., a spin- $\frac{1}{2}$ particle)	Optical cavity mode and two detectors
Local operations	Unitaries on each system	Interaction between cavity and detectors

two different orthogonal states depending on the two proper times involved in the protocol (see, e.g., Refs. [17,18]). We decided to employ this particular realization of our idea to underscore the relativistic aspect of our paper. One could propose an alternative mechanism to achieve a delay between two interactions, but such a mechanism would require external entities to manipulate the atoms and position them at specific times. Although this alternative mechanism could yield similar results, it would lack the relativistic nature. However, we would like to emphasize that the specifics of our model are not the focal point of our paper. Our main goal is to demonstrate that the violation of Bell inequalities is not always an unambiguous consequence of the indefinite temporal order of interactions.

The detector is a particle with two internal energy levels that (at the proper time specified by the clock) interacts with a quantum field confined in a cavity. We use the Unruh-DeWitt (UDW) detector model for the interaction; see Sec. IV A below and Appendix A for the details of the coupling.

Finally, the control is a spin- $\frac{1}{2}$ particle, whose two orthogonal spin states, $|\uparrow\rangle$ and $|\downarrow\rangle$, serve to define the molecules' trajectories (see, e.g., Ref. [19] for a realization of coherent spin-dependent trajectories which could be used here). Although each detector interacts with the cavity at the same proper time of its local clock, special-relativistic time dilation implies that the interactions take place at different coordinate times depending on the molecule's trajectory (which, in turn, depends on the spin).

In the protocol, the detectors in each molecule are prepared in their ground state $|g\rangle$ and the clocks are synchronized at a reference starting time τ_0 , while the spins of different molecules are prepared in an appropriate entangled state (defined below). Each molecule is sent to a cavity along a trajectory that depends on the spin. The clock triggers an interaction between the detector in the molecule and the field, creating entanglement between the two. (The proper time at which the interaction happens is chosen such that the molecule is in the cavity for either trajectory). At this point, the molecule is broken apart: the detector and the clock stay next to the corresponding cavity, while all the controls are brought together in a middle location. A joint measurement on the controls prepares an entangled state of the remaining systems, which can then be used to violate a Bell inequality.

In our setup, the target system on each side, say S_1 , comprises the field in the cavity as well as the two detectors that go through that cavity. Crucially, the field-detector interaction leaves the clock and control unaffected. This is important to ensure that each of the operations U^A, U^B acts only on the target system. Without this assumption, one could simply entangle each target system with an additional DoF, e.g., an extra particle, bring the two extra particles together, and, by

measuring them, induce entanglement on the two target systems. This would be a form of entanglement swapping [20] that does not require any control of time ordering (nor any control system for that matter).

Furthermore, note that since the control DoF goes through the cavity together with the rest of the molecule, we effectively need to trust the involved devices when we assume that the local operations leave the control untouched. This is the reason such a test for indefinite temporal order cannot be formulated in a device-independent way (just as in the gravitational protocol of Ref. [6]; see also discussion therein).

III. TRAJECTORIES

In this section, we will describe the trajectories of the molecules mentioned in the previous section. Building upon the concept presented in Sec. IA, we have made the decision to utilize the same trajectories in both wings of the experiment. This choice enables us to concentrate on one wing and its two molecules, thus facilitating the analysis of the significance of the trajectory's specific form in the overall protocol.

Each molecule has two possible trajectories, depending on the spin state. The specific trajectories we propose for one wing of the experiment are shown in Fig. 3, with identical choices for the other wing. Each molecule always starts and ends its trajectory at given events, which coincide for the two possibilities. However, the proper time elapsing along the two trajectories is different. Both trajectories can be constructed by joining four identical hyperbolic segments, characterized by proper accelerations $\mathcal{A}_\uparrow, \mathcal{A}_\downarrow$ for spin up, $|\uparrow\rangle$, or spin down, $|\downarrow\rangle$, respectively. These segments have to be rotated or flipped according to Fig. 3, so the acceleration for each trajectory switches signs three times. Let us assume that the acceleration for spin $|\uparrow\rangle$ is bigger than the acceleration for spin $|\downarrow\rangle$. Knowing the value of proper time along the generic hyperbolic trajectory (see, e.g., Ref. [21]), we can find the difference between proper times measured at the common end of one such pair of trajectories:

$$\Delta\tau = \underbrace{\frac{4}{\mathcal{A}_\downarrow} \operatorname{asinh}\left(\frac{\mathcal{A}_\downarrow T_A}{4}\right)}_{\tau_\downarrow} - \underbrace{\frac{4}{\mathcal{A}_\uparrow} \operatorname{asinh}\left(\frac{\mathcal{A}_\uparrow T_A}{4}\right)}_{\tau_\uparrow}, \quad (3)$$

where $\tau_{\uparrow/\downarrow}$ is the proper time measured along the trajectory of a \uparrow/\downarrow spin and T_A is the total travel time in a common inertial frame of reference, e.g., the frame used to initially synchronize the clocks.

Note that it is possible to achieve a large value of $\Delta\tau$ using a small value of proper acceleration. For a large value of T_A ,

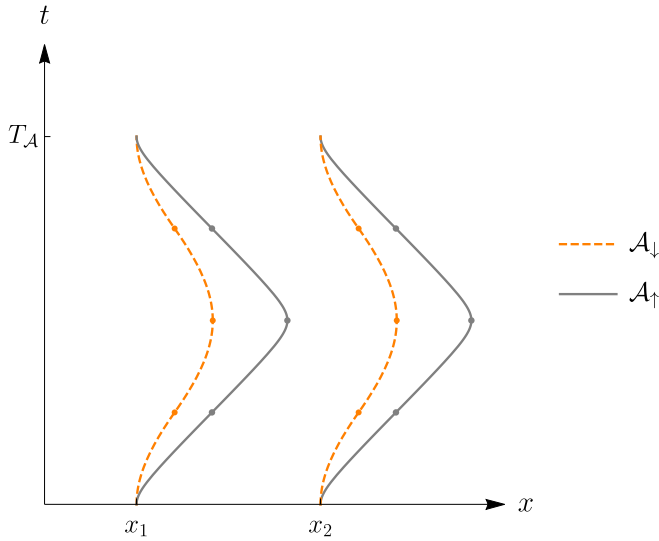


FIG. 3. Trajectories of the molecules in one cavity giving rise to the required time dilation. x_1, x_2 are initial positions of the molecules. The trajectory of each molecule depends on the spin of its particle called the control. For spin $|\uparrow\rangle$, the trajectory is described by the proper acceleration \mathcal{A}_\uparrow and analogously for spin $|\downarrow\rangle$. Dots along the trajectories divide each curve into four geometrically identical hyperbolic segments. The trajectories of the molecules in the second cavity are fully analogous.

we have

$$\Delta\tau = 2 \left(\frac{\ln\left(\frac{\mathcal{A}_\downarrow^2}{4}\right)}{\mathcal{A}_\downarrow} - \frac{\ln\left(\frac{\mathcal{A}_\uparrow^2}{4}\right)}{\mathcal{A}_\uparrow} \right) \quad (4)$$

$$+ 4 \left(\frac{1}{\mathcal{A}_\downarrow} - \frac{1}{\mathcal{A}_\uparrow} \right) \ln(T_{\mathcal{A}}) + O\left(\frac{1}{T_{\mathcal{A}}^2}\right). \quad (5)$$

It means that we can achieve the required $\Delta\tau$ (to make the events defined by such time dilated pair of clocks timelike) by accelerating for a long enough time, even for arbitrarily small accelerations. Finally, taking the initial state of the spin of the two molecules to be entangled, one of the two clocks in each cavity will be older than another in a correspondingly correlated manner. Thus, the order of operations, controlled by the clocks, will likewise be entangled, as a direct consequence of the initial spin entanglement and of time dilation. In this scenario, the joint spin state of the two molecules plays the role of the control, which is played by the position of a massive object in the gravitational case [6]. Table II summarizes the differences between the gravitational and our cavity-based implementation of the protocol, in terms of control systems, target(s), and local operations.

IV. PROTOCOL FOR INDEFINITE TEMPORAL ORDER

A. One cavity, two molecules

Before moving to the full protocol, let us consider the interaction between one cavity and a pair of molecules. In other words, let us focus only on one wing of the protocol. Each molecule contains, in addition to a clock and a control spin, a two-level detector, which interacts with the cavity via

the UDW Hamiltonian which in the Schrödinger picture has the following form (see also Appendix A):

$$\hat{H}_{\text{UDW}} = \lambda \chi_d(t) \hat{\mu}_S \hat{\phi}(x_d), \quad (6)$$

where λ is a dimensionless coupling constant; the real function $\chi_d(t)$ is equal to 0 when the detector does not interact and 1 for any other time and is commonly referred to as the switching function; $\hat{\mu}_S$ is the monopole operator $\hat{\mu}_S = \hat{\sigma}^+ + \hat{\sigma}^- = |g\rangle\langle e| + |e\rangle\langle g|$, where $|g\rangle$ is the ground state of the two-level system and $|e\rangle$ is its excited state. The Hilbert space spanned by $|g\rangle$ and $|e\rangle$ will be called the internal Hilbert space of the detector. Finally, $\hat{\phi}(x_d)$ is the field operator evaluated at the position of the detector.

At the beginning of the protocol, the cavity field is in the vacuum, denoted $|0\rangle$, and the two detectors are in their respective ground states. We synchronize the clocks, namely, we prepare them in the same state $|\tau_0\rangle$, and we prepare the two control spins in the entangled state $\frac{1}{\sqrt{2}}(|\uparrow\downarrow\rangle + |\downarrow\uparrow\rangle)$. After applying the spin-dependent accelerations described in Sec. III, the joint state of cavity and molecules is

$$\frac{1}{\sqrt{2}}(|\tau_\uparrow\tau_\downarrow\rangle|\uparrow\downarrow\rangle + |\tau_\downarrow\tau_\uparrow\rangle|\downarrow\uparrow\rangle)|gg\rangle|0\rangle, \quad (7)$$

where $|\tau_{\uparrow/\downarrow}\rangle$ is the state of the clock after it evolved for time $\tau_{\uparrow/\downarrow}$. Note that for later convenience, we have grouped the DoFs by type (clock, spin, detector) rather than by molecule. For example, instead of

$$\underbrace{|\tau_\uparrow\rangle|\uparrow\rangle|g\rangle}_{\text{1st molecule}} \otimes \underbrace{|\tau_\downarrow\rangle|\downarrow\rangle|g\rangle}_{\text{2nd molecule}}, \quad (8)$$

we write $|\tau_\uparrow\tau_\downarrow\rangle|\uparrow\downarrow\rangle|gg\rangle$, where inside each ket symbol we first write the state relative to molecule 1 and then the state relative to molecule 2.

We see from Eq. (7) that, after the spin-dependent accelerations, the clocks become entangled with the remaining systems. This can be problematic because, in the final protocol, we aim to observe entanglement in the target systems (detectors and cavities) after projecting the control on an appropriate state. Anything that correlates to the target, including the clocks, would effectively degrade entanglement. We can circumvent this by resynchronizing the clocks after they had passed through the cavity. This can be achieved, for example, by flipping the molecules' spins and imparting the accelerations identical to those in the first phase, whereby at the end, all the trajectories accrue equal proper times (this is analogous to the decorrelation of clocks in the gravitational scenario, discussed in Ref. [6]). This procedure allows us to ignore the clocks in the final state. Let us emphasize that the role of the clock is crucial to ensure events take place at a given time in the molecule reference frame so any conclusion about the order of events can be attributed to an intrinsic definition of events, similarly to the gravitational case¹. It is

¹One could also define the time of events relative to a common laboratory clock, and correlate the time of each event with a control degree of freedom. This would be effectively like “simulating” time dilation by a direct de-synchronisation of clocks. However, here we are interested in a relativistic definition of events and event order.

only after ensuring that the clock decorrelates from the rest of the system that we can remove it from the description. Therefore, after tracing out the clock DoFs, we simplify the notation and map $|\tau_{\uparrow/\downarrow}\rangle|\uparrow/\downarrow\rangle \mapsto |\uparrow/\downarrow\rangle$, which allows us to denote the state (7) as

$$|\Psi_0^1\rangle = \frac{1}{\sqrt{2}}(|\uparrow\downarrow\rangle + |\downarrow\uparrow\rangle)|gg\rangle|0\rangle, \quad (9)$$

where the subscript 0 informs us that this is the initial state of the system (before detectors and the cavity interact) and the index 1 in the superscript informs us that this is the state of the field and two molecules in wing 1 (see Fig. 2).

Note that according to the scheme presented above, state $|\uparrow\downarrow\rangle$ corresponds to the case when the detector at position x_2 is the first to interact with the cavity (the spin of the molecule that interacts earlier is \downarrow). Similarly, for state $|\downarrow\uparrow\rangle$, the detector at x_1 interacts earlier than the detector at x_2 . In further calculations, we assume that the duration T of each detector's interaction with the cavity is smaller than the time dilation between the two trajectories, i.e., $T \leq \Delta\tau$, to ensure that the two detectors do not interact simultaneously from the perspective of the cavity's reference frame.

The interaction between each detector and the cavity is described by Eq. (A5) from Appendix A, therefore since the order of interactions is given by the molecule's spin, we can write the final state in the form

$$|\Psi^1\rangle = \frac{1}{\sqrt{2}}(|\uparrow\downarrow\rangle\hat{U}_1\hat{U}_2|g\rangle|g\rangle|0\rangle + |\downarrow\uparrow\rangle\hat{U}_2\hat{U}_1|g\rangle|g\rangle|0\rangle). \quad (10)$$

Here, operators \hat{U}_1 and \hat{U}_2 act on the internal states of the first (left) and the second (right) detector, respectively. For ease of notation we define the state $|\psi_R\rangle := \hat{U}_1\hat{U}_2|g\rangle|g\rangle|0\rangle$, where the subscript R denotes that the right (second) detector interacts before the left (first) one, and analogously define $|\psi_L\rangle := \hat{U}_2\hat{U}_1|g\rangle|g\rangle|0\rangle$. We thus have

$$|\Psi^1\rangle = \frac{1}{\sqrt{2}}|\uparrow\downarrow\rangle|\psi_R\rangle + \frac{1}{\sqrt{2}}|\downarrow\uparrow\rangle|\psi_L\rangle. \quad (11)$$

Using the evolution operator given by Eq. (A5) from Appendix A, we find an explicit form of $|\psi_R\rangle$, $|\psi_L\rangle$, up to leading order in the interaction parameter λ using Eq. (A9) from Appendix A. The results of this calculation are

$$|\psi_R\rangle = |gg\rangle|0\rangle + |ge\rangle|\phi_{ge}^R\rangle + |eg\rangle|\phi_{eg}^R\rangle + O(\lambda^2), \quad (12)$$

$$|\psi_L\rangle = |gg\rangle|0\rangle + |ge\rangle|\phi_{ge}^L\rangle + |eg\rangle|\phi_{eg}^L\rangle + O(\lambda^2), \quad (13)$$

where $|\phi_{ge}^{L/R}\rangle$ and $|\phi_{eg}^{L/R}\rangle$ are first order in λ , describing field states containing a single excitation, see Appendix B for their explicit expression.

B. Two cavities, four molecules

We now move to the full protocol, whose aim is to explicitly demonstrate indefinite temporal order. We consider two wings of the experiment, where in each wing two operations take place (see Fig. 2). The goal is to correlate the order of each pair of operations with a control system and, after measuring the control, produce an entangled state between the two wings, which would not have been possible had the operations been realized in a definite order.

Recall that we want to entangle the target systems which comprise the fields in both cavities as well as the detectors (which are two per cavity), while the four spin- $\frac{1}{2}$ particles play the role of the control. The full protocol involves four molecules (two in each wing), where each molecule contains a clock, a detector, and a spin- $\frac{1}{2}$ particle. Initially, the state of these molecules reads

$$|\tau_0\tau_0\tau_0\tau_0\rangle \frac{1}{\sqrt{2}}(|\uparrow\downarrow\uparrow\downarrow\rangle + |\downarrow\uparrow\downarrow\uparrow\rangle)|gggg\rangle, \quad (14)$$

where $|\tau_0\rangle$ is the initial state of one clock (and thus all four clocks are initially decorrelated and synchronized) and each detector is in its ground state, while the spins are entangled.

Note that this state is constructed in such a way that the four molecules can be divided into two identical pairs. As we explained before, we have two wings of the experiment in which we have analogous trajectories of the molecules. These pairs are then accelerated as explained in Sec. III. After the process of acceleration, the state of all four molecules is

$$\frac{1}{\sqrt{2}}(|\tau_{\uparrow}\tau_{\downarrow}\tau_{\uparrow}\tau_{\downarrow}\rangle|\uparrow\downarrow\uparrow\downarrow\rangle + |\tau_{\downarrow}\tau_{\uparrow}\tau_{\downarrow}\tau_{\uparrow}\rangle|\downarrow\uparrow\downarrow\uparrow\rangle)|gggg\rangle. \quad (15)$$

Due to time dilation, after the acceleration takes place, one clock from each pair of molecules will be older than the other from the same pair. We cannot determine which one because the initial state of spins is a superposition of two different possibilities. Next, each pair of molecules enters a cavity. The first pair is placed in cavity 1 at the respective positions x_1 and x_2 (determined relative to the boundary of this cavity at $x = 0$). The second pair of molecules is placed in cavity 2 at the same positions relative to that cavity. Recall that the field in each cavity is initially in the vacuum state. As discussed in the previous section, we can decorrelate the clock DoF by resynchronizing the clocks. This is done after the molecules interact with the cavities. To keep track of the effect of the clocks on the detector-field interactions, it is enough to note that a detector belonging to a molecule with spin \downarrow interacts first (and with spin \uparrow interacts second). To sum up the protocol, the initial state of the total system including the two cavities is

$$|\Psi_0^{\text{tot}}\rangle = \frac{1}{\sqrt{2}}(|\uparrow\downarrow\uparrow\downarrow\rangle + |\downarrow\uparrow\downarrow\uparrow\rangle)|\underbrace{gg\rangle|0\rangle}_{\in S_1} \otimes |\underbrace{gg\rangle|0\rangle}_{\in S_2}\rangle, \quad (16)$$

where we used \otimes to separate states from the two cavities and showed which DoFs comprise the targets S_1 and S_2 introduced in Sec. I.

After the interactions between the detectors and the cavity fields, the state of the system reads

$$|\Psi^{\text{tot}}\rangle = \frac{1}{\sqrt{2}}(|\uparrow\downarrow\uparrow\downarrow\rangle|\psi_R\rangle \otimes |\psi_R\rangle + |\downarrow\uparrow\downarrow\uparrow\rangle|\psi_L\rangle \otimes |\psi_L\rangle), \quad (17)$$

where the detectors and cavity states, $|\psi_{L/R}\rangle$, are those in Eqs. (12) and (13).

Next, the molecules are broken apart. All spins are sent to a common location where, at an event labeled D , they are jointly measured in the basis $\frac{1}{\sqrt{2}}(|\uparrow\downarrow\uparrow\downarrow\rangle \pm |\downarrow\uparrow\downarrow\uparrow\rangle)$. This prepares the remaining systems—cavities and detectors (which stay

next to their cavities)—in the state

$$|\Psi^\pm\rangle = \frac{1}{\sqrt{2}}(|\psi_R\rangle \otimes |\psi_R\rangle \pm |\psi_L\rangle \otimes |\psi_L\rangle), \quad (18)$$

where the sign \pm depends on the measurement outcome. This state is entangled as long as $|\psi_L\rangle \neq |\psi_R\rangle$. This is typically shown by finding the scalar product between $|\psi_L\rangle$ and $|\psi_R\rangle$, which requires the Dyson series up to second order in λ .

However, there is an equivalent but technically much simpler method to show that the final state is in general entangled, which is to consider another measurement performed on each detector pair in a basis containing the vector $1/\sqrt{2}(|ge\rangle + |eg\rangle)$. The resulting conditional states of the fields [arising from Eqs. (12) and (13)] read

$$\frac{1}{\sqrt{2}}(\langle ge| + \langle eg|)|\psi_R\rangle = \frac{1}{\sqrt{2}}(|\phi_{ge}^R\rangle + |\phi_{eg}^R\rangle) + O(\lambda^3), \quad (19)$$

$$\frac{1}{\sqrt{2}}(\langle ge| + \langle eg|)|\psi_L\rangle = \frac{1}{\sqrt{2}}(|\phi_{ge}^L\rangle + |\phi_{eg}^L\rangle) + O(\lambda^3), \quad (20)$$

where the order of this result, i.e., $O(\lambda^3)$, is explained in Appendix D. To sum up this method: One can perform a measurement on each pair of detectors in the basis $1/\sqrt{2}(|ge\rangle + |eg\rangle)$ to obtain the state of the field given in Eqs. (19) and (20), and then follow the previously explained procedure, i.e., measure the control. Upon measuring the control in the entangled basis, $\frac{1}{\sqrt{2}}(|\uparrow\downarrow\uparrow\downarrow\rangle \pm |\downarrow\uparrow\downarrow\uparrow\rangle)$, the joint state of two cavities consists only of the field states because all other DoFs were measured. This state of the fields, up to the leading order

in λ , is

$$\begin{aligned} |\tilde{\Psi}^\pm\rangle \propto & \underbrace{(|\phi_{ge}^R\rangle + |\phi_{eg}^R\rangle)}_{|\Phi_R\rangle} \otimes \underbrace{(|\phi_{ge}^R\rangle + |\phi_{eg}^R\rangle)}_{|\Phi_R\rangle} \\ & \pm \underbrace{(|\phi_{ge}^L\rangle + |\phi_{eg}^L\rangle)}_{|\Phi_L\rangle} \otimes \underbrace{(|\phi_{ge}^L\rangle + |\phi_{eg}^L\rangle)}_{|\Phi_L\rangle}. \end{aligned} \quad (21)$$

The conditional state of the fields $|\tilde{\Psi}^\pm\rangle$ is entangled as long as $|\Phi_R\rangle \neq |\Phi_L\rangle$ which is easier to verify than the condition $|\psi_R\rangle \neq |\psi_L\rangle$. We further note that the measurement on the detectors has different possible outcomes, not all of which result in entangled field states. Crucially, however, for a product state across S_1 and S_2 , all local detector measurements would result in product states of the fields. Therefore, obtaining an entangled state for one of the outcomes is sufficient to prove that the original state was entangled.

To sum up, we have shown that using two cavities, four molecules, and the basic effects of special relativity, we can obtain the state given in Eq. (21). If this state is entangled, in the next steps of the protocol this entanglement can be used to violate Bell's inequalities with the goal to prove that the detector–field interaction events were not classically ordered.

C. Entanglement of the final state

We now proceed to prove that the state in Eq. (21) can indeed be entangled by showing that there exist parameters for which $|\Phi_R\rangle \neq |\Phi_L\rangle$. The scalar product between these states reads

$$\langle\Phi_R|\Phi_L\rangle = \frac{\sum_k \frac{e^{-i\Delta\tau(\omega_k+\Omega)}}{(\omega_k+\Omega)^2} [1 - \cos(T(\omega_k + \Omega))](u_k(x_1) + e^{i\Delta\tau(\omega_k+\Omega)}u_k(x_2))^2}{2 \sum_n \frac{\sin^2 \frac{T(\omega_n+\Omega)}{2}}{(\omega_n+\Omega)^2} [u_n(x_2)^2 + 2u_n(x_2)u_n(x_1) \cos(\Delta\tau(\omega_n + \Omega)) + u_n(x_1)^2]}. \quad (22)$$

The explicit derivation is presented in Appendix C. Therein, we further show how to choose parameters for which the states are not just different but orthogonal. To summarize this procedure, the parameters that have to be chosen are:

- (1) The length L of each cavity and the positions x_1, x_2 of the molecules relative to their respective cavity.
- (2) The energy gap Ω of the detectors.
- (3) The duration T of the interaction between each detector and the cavity field.
- (4) The time dilation $\Delta\tau$ between clocks within each pair of molecules (within each cavity), arising from the different accelerations $\mathcal{A}_{\uparrow/\downarrow}$.

Remarkably, it is also possible to find parameters such that $|\Phi_R\rangle \neq |\Phi_L\rangle$ even when the two field-detector interactions within each cavity are spacelike separated, see Fig. 4. This means that it is possible to obtain an entangled state also in the case when, in some reference frame, the relevant operations are performed in the same temporal order. Although from the perspective of such a reference frame, the operations would take place over four different coordinate regions, their order would be the same in each of the amplitudes. Obviously then, entanglement generated in this scheme cannot be

simply attributed to nonclassical temporal order. We discuss implications and argue for the generality of this result in the next sections.

D. Ambiguity in the signature of indefinite temporal order

We have explicitly modeled a special-relativistic version of a protocol where gravitational time dilation and quantum superposition lead to an indefinite temporal order of events from Ref. [6]. This protocol was formulated in terms of a Bell inequality for temporal order. The idea was to formulate a protocol where operations in a *definite* order cannot produce an entangled state if an appropriate set of assumptions is satisfied. (The final step of the protocol requires measurements on the state to violate a Bell inequality and verify the entanglement.) The motivation was to find a test of temporal order that is *theory independent*, which was based on the observation that a violation of a Bell inequality would prove indefinite temporal order without assuming that the final state is described by quantum mechanics. In this section, we re-examine the assumptions made in Ref. [6], showing that the theory-independent nature of the argument is problematic.

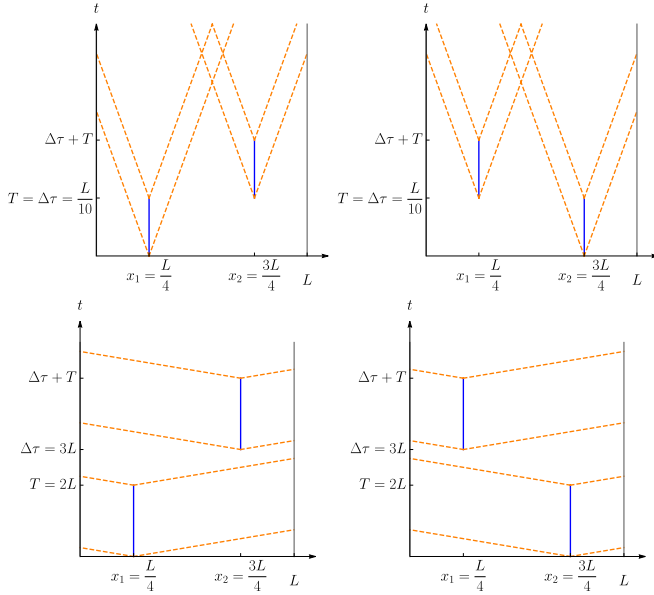


FIG. 4. Space-time diagrams of interacting detectors. Space-time diagram showing the regions where the detector-field interactions lead to an entangled state, Eq. (21). The diagrams are for one cavity—the interaction regions are identically defined for the second cavity. The first row shows spacelike separated regions which nevertheless yield entanglement. The second row shows timelike separation, which yields maximal entanglement. The columns correspond to the two amplitudes of the process that are superimposed using the control (spin) state. See Appendix C for the supporting calculations.

We first remark that the issue we have identified does not arise if we believe that quantum mechanics is valid, i.e., if we wish to provide experimental evidence for nonclassical temporal order assuming that the involved states and transformations are faithfully described by quantum theory. In such a case, already the one-cavity part of our protocol, Sec. IV A, or the gravitational equivalent, is sufficient. The reason is that, at an abstract level, these protocols implement a quantum switch [3]—a scenario where two local operations, represented by unitary operators \hat{U}^A , \hat{U}^B , act on a target system in an order determined by a control system which is prepared in a superposition, thus producing a final state of the form

$$|\psi_{\text{fin}}\rangle = \frac{1}{\sqrt{2}}(|0\rangle\hat{U}^A\hat{V}_0\hat{U}^B + |1\rangle\hat{U}^B\hat{V}_1\hat{U}^A)|\psi\rangle. \quad (23)$$

Here, $|0\rangle$, $|1\rangle$ are two basis states of the control, and $|\psi\rangle$ is the initial state of the target system. \hat{V}_0 and \hat{V}_1 are two arbitrary unitary operators, representing the evolution of the target between the two operations. Most presentations of the switch do not include the intermediate evolution, but we will see shortly that this is important in our context². Given an implementation of the switch, by making appropriate final measurements for a set of suitably chosen operations \hat{U}^A , \hat{U}^B , it is possible to prove that the operations are not performed in a

definite order. This procedure is known as measuring a *causal witness* [22,23] and it could, in principle, be incorporated within a single-cavity variant of our protocol to demonstrate that, if the quantum description of the experiment is correct, the cavity-detector interactions do not take place in a definite order.

Returning to the Bell inequality approach, it essentially is an entangled version of the switch, with the final state of the form

$$|\psi_{\text{fin}}\rangle = \frac{1}{\sqrt{2}}(|0\rangle\hat{U}^{A_1}\hat{V}_0\hat{U}^{B_1}|\psi\rangle \otimes \hat{U}^{A_2}\hat{V}_0\hat{U}^{B_2}|\psi\rangle + |1\rangle\hat{U}^{B_1}\hat{V}_1\hat{U}^{A_1}|\psi\rangle \otimes \hat{U}^{B_2}\hat{V}_1\hat{U}^{A_2}|\psi\rangle). \quad (24)$$

To use such a state to disprove classical temporal order among \hat{U}^A , \hat{U}^B , the state has to arise in a scenario satisfying all assumptions used to derive the Bell inequality for temporal order, apart from the assumption of classical order itself. All assumptions used in Ref. [6] for the derivation of the inequality are the initial state of the target systems S_1 , S_2 is separable; transformations performed on the targets are local (i.e., the operations on target S_j act as identity on other DoFs of the system); events and space-time regions at which transformations and measurements take place are suitably separated: both interaction events in one wing are spacelike separated from both interaction events in the other wing; and event D is spacelike from the events at which the Bell measurements are performed (which as, usual in Bell inequalities, are assumed to be spacelike from each other); the choices of bases for Bell measurements are independent of all other aspects of the experiment (often referred to as free choice assumption); and, finally, of course, the assumption that events at which transformations and measurements are performed are classically ordered.

The surprising result identified in Sec. IV C is that entanglement is produced while *all* the above assumptions are met, including the assumption of classical order. Clearly, some other assumption was made to derive the inequality and is violated in our implementation. Indeed, as already mentioned, the additional implicit assumption made in Ref. [6] is that the target systems do not have nontrivial evolution apart from the transformations \hat{U}^A and \hat{U}^B . Below we explain why this assumption is violated in the present implementation and in Sec. IV D we argue that this will remain true in a generic dynamical implementation. As a result, our considerations are valid for any generic scheme attempting to verify the indefinite temporal order of events implemented in a fully quantum mechanical manner.

To see where the assumption of no free evolution enters and why it is the culprit, it is again sufficient to look at one wing of our setup. Comparing a single-cavity scenario, Eq. (10), and a generic quantum switch, Eq. (23), one finds that the evolution operators \hat{U}_1 , \hat{U}_2 in Eq. (10) are not directly representing the local operations \hat{U}^A , \hat{U}^B . The reason is that \hat{U}_1 , \hat{U}_2 are written in the Dirac (interaction) picture, which necessarily includes time evolution with respect to the free Hamiltonian (starting from some initial time established in a common reference frame). By unraveling this time evolution, one finds precisely a state of the form (23), where \hat{V}_0 and \hat{V}_1 represent the free evolution of the targets (i.e., cavity and detectors) between the

²For generality, one can also include a control-dependent initial state, but this is not necessary for our analysis.

interactions. Note that the time intervals between the events, and thus intervals of free evolution, are equal in the reference frame of the cavity, which means that in that frame, $\hat{V}_0 = \hat{V}_1$. On the other hand, \hat{U}^A, \hat{U}^B describe *only* the field-cavity interactions in the Schrödinger picture³.

The reason this is relevant here is that if the free Hamiltonian does not commute with the interaction, the free evolution does not commute with \hat{U}^A, \hat{U}^B , and this is how the presence of entanglement can be explained in the state in Eq. (24) in a frame where $\hat{V}_0 = \hat{V}_1$ and the events are spacelike separated. Note that in that case there is a reference frame where $A_j < B_j$ for both states of the control, however, as we mentioned above, in that frame necessarily $\hat{V}_0 \neq \hat{V}_1$, since the time intervals of free evolution along the worldlines of molecules 1 and 2 are in such a frame necessarily different. In such a frame, the final state in the two-wing scenario becomes

$$|\psi_{\text{fin}}\rangle = \frac{1}{\sqrt{2}}(|0\rangle\hat{U}^{B_1}\hat{V}_0\hat{U}^{A_1}|\psi\rangle \otimes \hat{U}^{B_2}\hat{V}_0\hat{U}^{A_2}|\psi\rangle + |1\rangle\hat{U}^{B_1}\hat{V}_1\hat{U}^{A_1}|\psi\rangle \otimes \hat{U}^{B_2}\hat{V}_1\hat{U}^{A_2}|\psi\rangle), \quad (25)$$

and the presence of entanglement is thus interpreted as due to overall different dynamics depending on the control, $\hat{U}^{B_1}\hat{V}_0\hat{U}^{A_1} \neq \hat{U}^{B_1}\hat{V}_1\hat{U}^{A_1}$, i.e., in that frame while the order of operations is common, when they take place relative to periods of free dynamics, and thus the overall evolution, depends on the control. Crucially, in this case, temporal order among events cannot even be defined as it depends on the reference frame. A further discussion of the role played by free evolution in this protocol is presented in the next section.

In fact, if free evolution and the applied operations do not commute, even simpler scenarios can illustrate the issue. Consider that one of the operations is trivial, say $\hat{U}^B = \hat{\mathbb{1}}$, and so, in fact, only *one* operation is applied. The noncommutativity between \hat{U}_A and $\hat{V} = \hat{V}_0 = \hat{V}_1$ (we are in the reference frame of the cavity) would again result in different final states depending on when \hat{U}^A is applied relative to \hat{V} . This would again lead to an entangled final state in a two-wing scenario, even though in this case there is no time order of events to speak of.

Finally, we note that in all quantum switch scenarios, including the entangled switch, there is an assumption that each local operation is performed only once. This condition is, however, naturally satisfied in relativistic implementations such as ours, as each operation is performed at a specific time of a local clock.

We have focused so far on a particular realization of the entangled switch protocol—with two-level detectors and cavity-confined quantum field modes as targets, and the position DoFs of the detectors as the control. However, our main result and its explanation applies to any physical realization of the protocol. Indeed, we have shown that entanglement can be generated for spacelike separated operations and identified

that this is due to the free evolution of the targets. For any physical implementation of the protocol, if the applied operations do not commute with the free evolution, the final state will, in general, be entangled regardless of the commutation relations between the operations themselves, and thus also regardless of their temporal order. Entanglement can arise even if only one operation is applied, as discussed in the previous section.

E. Entanglement generation for spacelike events and its implications

Results from the previous section show that also for spacelike separation of the interaction events, Bell's inequality for temporal order can be violated. This statement seems paradoxical because for spacelike separated events we cannot define their temporal order—it depends on the reference frame. Here we look more closely at the compatibility of this fact with the locality of evolution.

Let us consider the cavity and two molecules placed near its boundaries. We know that entanglement at spacelike separation appears for a short time of interaction and small time dilation (see Fig. 4). By definition, in such scenarios, information about the interaction with the field cannot be transferred from the first to the second detector before the latter interacts with the field. To notice the problem with this situation, we can split the whole cavity into three parts (see Fig. 5). Let us denote these as F_L, F , and F_R . The field F_L refers only to the part of the cavity near the left detector and, similarly, F_R describes just the right part of the cavity. The field F refers to the middle of the whole cavity. The lengths of each part are chosen to make sure that information about interaction with the left (right) molecule can be localized only within the left (right) part of the cavity. Because of this division of the cavity into three parts, we can capture the two alternative orders of events as follows.

For one order, the left molecule interacts first, $L < R$; for the other, the right molecule interacts first, $R < L$. The whole evolution \hat{U} of the system containing two molecules and three parts of the cavity can then be presented as $\hat{U} = \hat{U}_3\hat{U}_2\hat{U}_1$, where

- (1) \hat{U}_1 : interaction of the left (right) molecule with F_L (F_R) and free evolution of remaining parts.
- (2) \hat{U}_2 : free evolution of the whole cavity.
- (3) \hat{U}_3 : interaction of the right (left) molecule with the F_R (F_L) and free evolution of remaining parts.

The two scenarios appear to differ only by the order of events at which detectors and the field interact. If these events are spacelike, from the original argument, one would not expect any difference between the two scenarios. However, the free evolution always contains parts that are timelike to one of the interaction events and, in general, the three evolution operators do not commute.

Thus, despite the spacelike separation of the interaction events, the free part of the evolution still affects the system and results in a different state of the targets for the two wings of the protocol. It means that for such a case we cannot argue that violation of Bell's inequalities implies indefinite order of events because we violate the additional assumption: there is an additional part of the evolution of the target systems and

³Strictly speaking, we should add free-evolution operators also before and after the two local unitaries—not only in between. However, free evolution acts trivially on the vacuum state (our initial state), while the final evolution can be reabsorbed in the definition of the measurement basis.

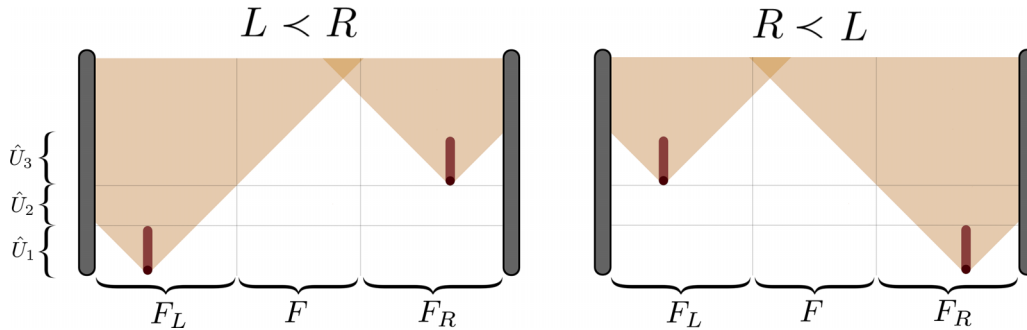


FIG. 5. Space-time diagram of a cavity interacting with two detectors. Operators \hat{U}_1 and \hat{U}_3 describe the evolution of the system according to the interaction, and \hat{U}_2 is an operator of the free evolution that occurs between interactions. F_L and F_R are parts of the cavity that can interact with the detector in some finite time. F is a middle segment of the cavity that evolves only due to the free evolution operator between interactions.

it is this evolution that causes a different final state despite spacelike separation of the events at which the interactions defining the order take place.

However, we claim that this assumption is unavoidable in a generic realization of the studied protocol, also including its gravitational version. Indeed, it is of course possible to identify implementations where the assumption of no free evolution of the targets does hold (e.g., with polarization or angular momentum DoFs of photons) or where the operations are performed within a degenerate subspace of the Hamiltonian of the targets (and thus commute with free evolution), so only noncommutativity between the two local operations is relevant. And such strategies would lead to an entangled final state only if the local operations are timelike and applied in a nonclassical order. However, identifying such implementations does require a theoretical description of the states and dynamics of the involved systems. In other words, one needs theory-dependent assumptions to interpret a violation of the final Bell inequalities as a signature of indefinite temporal order, while seeking a theory-independent way to certify nonclassical time order was one of the key motivations of Ref. [6].

Furthermore, the observation above does not depend on the special-relativistic setting studied in this paper and equally holds for gravitational protocols. Indeed, nothing in our argument depends on how the time dilation of the clocks is achieved. For example, the position of a massive body can determine—through gravitational time dilation—the time at which a single operation takes place (relative to some mass-independent coordinates). This can lead to the same situation described earlier: the creation of entanglement (in a two-wing scenario) even with a single operation per wing. Again, theory-dependent assumptions would be required to ensure that entanglement can only arise as a result of an indefinite order of events.

V. CONCLUSION

In this paper, we constructed a nongravitational scenario where accelerating particles, interacting with quantum fields, according to their own internal clock DoFs, can lead to a violation of the temporal Bell inequalities analogous to the gravitational case. In Sec. II, we introduced the formalism required to reproduce the gravitational protocol using special

relativistic time dilation. We defined the kinematics of all particles involved in the protocol and the appropriate coupling between them and the quantum field. In Sec. IV, we discussed the full protocol that explicitly demonstrated a violation of Bell's inequalities, which are claimed to test the indefinite temporal order of events. We described the procedure that would lead us to the violation of Bell's inequalities for the proposed system that also occurs when the events responsible for the entanglement are spacelike, which we interpreted as an ambiguity in the signature of indefinite temporal order. We finally found that this surprising conclusion is the result of the failure of the additional assumption that target systems have no other evolution except the one governed by unitaries applied in a specific time order. We presented a detailed discussion of this problem in the last two sections of our paper.

We argued that to satisfy all assumptions of the Bell theorem for time order—including the auxiliary one (of no free evolution of the targets)—it is essential to invoke theory-dependent arguments. What is more, in a generic implementation—including a gravitational version of the protocol—this assumption is not met. Our chosen model thus serves as a means to clarify the overlooked aspect of Bell inequalities for temporal order. Consequently, our conclusions hold significance for any theoretical or experimental pursuit of indefinite temporal order.

Being able to describe and experimentally test entangled temporal order (i.e., even working fully within quantum mechanics) is of interest in its own right. Our result, however, opens the question of whether it is possible to formulate a stronger, theory-independent, test of temporal order. The insight from the present paper is that it is problematic to separate out the effect of the free dynamics of the system from that of the local operations. A possible avenue to circumvent this is to consider more general operations than the fixed unitaries discussed thus far: they can involve a measurement of the system, producing a classical variable as the outcome. Furthermore, a setting variable for each party can model a choice among different operations. In this fashion, one can consider directly the causal relations between parties—understood operationally as correlations between settings and outcomes—without relying on a theory-dependent description of the transformations. We leave further investigation of this possibility to future work.

ACKNOWLEDGMENTS

K.D. is financially supported by the (Polish) National Science Center Grant No. 2021/41/N/ST2/01901. F.C. acknowledges support through the Australian Research Council (ARC) DECRA Grant No. DE170100712, M.Z. acknowledges support through the ARC Future Fellowship Grant No. FT210100675 and the Knut and Alice Wallenberg foundation through a Wallenberg Academy Fellowship No. 2021.0119; F.C. and M.Z. acknowledge support through ARC Centre of Excellence EQuS CE170100009. Nordita is supported in part by NordForsk. The University of Queensland (UQ) acknowledges the Traditional Owners and their custodianship of the lands on which UQ operates.

APPENDIX A: UNRUH-DEWITT COUPLING

In this Appendix, we define the interaction between a two-level system, the detector, and the scalar field inside the cavity via the pointlike UDW Hamiltonian [24,25]. We first discuss key properties of the field operators. We consider a scalar field of a mass m governed by the Klein-Gordon equation⁴,

$$(\square + m^2)\phi = 0, \quad (\text{A1})$$

in a cavity of length L fulfilling Dirichlet boundary conditions, $\phi(x=0) = \phi(x=L) = 0$. The field has the following mode solutions:

$$u_n(x, t) = \frac{1}{\sqrt{\omega_n L}} \sin(k_n x) e^{-i\omega_n t} \equiv u_n(x) e^{-i\omega_n t}, \quad (\text{A2})$$

where $\omega_n = \sqrt{k_n^2 + m^2}$, $k_n = \frac{n\pi}{L}$, $n \in \mathbb{N}$. Using these modes, the field operator $\hat{\phi}$ can be decomposed as

$$\hat{\phi}(x) = \sum_n [\hat{a}_n^\dagger u_n(x) + \hat{a}_n u_n(x)], \quad (\text{A3})$$

where \hat{a}_n and \hat{a}_n^\dagger are annihilation and creation bosonic operators satisfying the canonical commutation relations, $[\hat{a}_n, \hat{a}_k^\dagger] = \delta_{nk}$ and $[\hat{a}_n, \hat{a}_k] = [\hat{a}_n^\dagger, \hat{a}_k^\dagger] = 0$. For the detector, we consider a two-level system, the simplest model of an atom, with an energy gap Ω , and position parameter denoted x_d . (where the subscript d hereafter stands for the detector). The full Hamiltonian consists of the free Hamiltonians of the scalar field and the detector, and an interaction Hamiltonian. One of the simplest choices of the interaction between a scalar field and a two-level system is the pointlike UDW Hamiltonian which, in the Schrödinger picture, has the following form:

$$\hat{H}_{\text{UDW}} = \lambda \chi_d(t) \hat{\mu}_S \hat{\phi}(x_d), \quad (\text{A4})$$

⁴For generality, we write everything for arbitrary m , although in the numerical calculations below we set $m = 0$.

APPENDIX B: DETAILS OF CALCULATIONS OF THE FINAL STATE

Using the form of the evolution operator (A5) we can find that

$$|\psi_R\rangle = \hat{U}_1 \hat{U}_2 |g\rangle |g\rangle |0\rangle = |g\rangle |g\rangle |0\rangle - i\lambda \int dt_2 \chi_{2R}(t_2) \sum_k \frac{1}{\sqrt{\omega_k L}} e^{i(\omega_k + \Omega)t_2} \sin\left(\frac{k\pi}{L} x_2\right) |g\rangle |e\rangle \hat{a}_k^\dagger |0\rangle$$

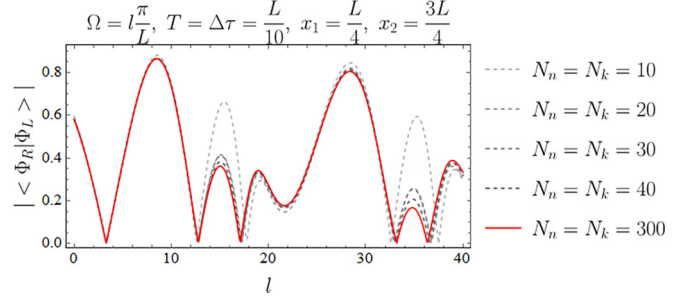


FIG. 6. The analysis of an orthogonality between $|\Phi_L\rangle$ and $|\Phi_R\rangle$. The absolute value of the scalar product as a function of the energy gap of the detector Ω .

where λ is a dimensionless coupling constant; the real function $\chi_d(t)$ is equal to 0 when the detector does not interact and 1 for any other time and is commonly referred to as the switching function; $\hat{\mu}_S$ is the monopole operator $\hat{\mu}_S = \hat{\sigma}^+ + \hat{\sigma}^- = |g\rangle\langle e| + |e\rangle\langle g|$, where $|g\rangle$ is the ground state of the two-level system and $|e\rangle$ is its excited state. The Hilbert space spanned by $|g\rangle$ and $|e\rangle$ will be called the internal Hilbert space of the detector. Finally, $\hat{\phi}(x_d)$ is the field operator evaluated at the position of the detector. As mentioned above, the full Hamiltonian also includes the time-independent free Hamiltonian of the field and of the two-level system, which reads $\hat{H}_0 = \sum_n \omega_n \hat{a}_n^\dagger \hat{a}_n \otimes \mathbb{1} + \mathbb{1} \otimes \Omega \hat{\sigma}^+ \hat{\sigma}^-$. Thus, the evolution of the state of the full system in the Dirac picture (also called the interaction picture) is here given by the unitary of the form

$$\hat{U} = \mathcal{T} \exp -i \int_{-\infty}^{\infty} dt \hat{H}_{\text{UDW}}^{(D)}(t), \quad (\text{A5})$$

where (D) stands for the Dirac picture and \mathcal{T} is the time-ordering operator. It can be shown that [26]

$$\hat{H}_{\text{UDW}}^{(D)}(t) = \chi(t) \lambda \hat{\mu}^{(D)} \hat{\phi}^{(D)}, \quad (\text{A6})$$

where

$$\hat{\mu}^{(D)} = (e^{i\Omega t} \hat{\sigma}^+ + e^{-i\Omega t} \hat{\sigma}^-), \quad (\text{A7})$$

$$\hat{\phi}^{(D)}(x_d) = \sum_n (\hat{a}_n^\dagger u_n(x_d) e^{i\omega_n t} + \text{H.c.}). \quad (\text{A8})$$

The evolution operator (A5) can be expanded into the Dyson series. For a sufficiently small value of the coupling constant λ , we can limit this series to the first-order term. We further show in Appendix B that the next contributing term is λ^3 . Thus, in the above approximation:

$$\begin{aligned} \hat{U} &= \mathbb{1} - i\lambda \int_{-\infty}^{\infty} dt \chi_d(t) (e^{i\Omega t} \hat{\sigma}^+ + e^{-i\Omega t} \hat{\sigma}^-) \\ &\times \sum_n (\hat{a}_n^\dagger u_n(x_d) e^{i\omega_n t} + \hat{a}_n u_n(x_d) e^{-i\omega_n t}). \end{aligned} \quad (\text{A9})$$

$$-i\lambda \int dt_1 \chi_{1R}(t_1) \sum_k \frac{1}{\sqrt{\omega_k L}} e^{i(\omega_k + \Omega)t_1} \sin\left(\frac{k\pi}{L}x_1\right) |e\rangle |g\rangle \hat{a}_k^\dagger |0\rangle + O(\lambda^2), \quad (\text{B1})$$

where χ_{1R} -switching function for the first detector in the case that the right detector interacts before the left one, χ_{2R} -switching function for the second detector in the case that the right detector interacts earlier. We assume that the interaction starts and ends rapidly, so $\chi_{2R}(t) = 1$ for $t \in (0, T)$ and $\chi_{2R}(t) = 0$ for any other time. Similarly, $\chi_{1R}(t) = 1$ for $t \in (\Delta\tau, \Delta\tau + T)$ and $\chi_{1R}(t) = 0$ for any other time. We can proceed with the same calculation for $|\psi_L\rangle$,

$$\begin{aligned} |\psi_L\rangle &= \hat{U}_2 \hat{U}_1 |g\rangle |g\rangle |0\rangle = |g\rangle |g\rangle |0\rangle - i\lambda \int dt_2 \chi_{2L}(t_2) \sum_k \frac{1}{\sqrt{\omega_k L}} e^{i(\omega_k + \Omega)t_2} \sin\left(\frac{k\pi}{L}x_2\right) |g\rangle |e\rangle \hat{a}_k^\dagger |0\rangle \\ &- i\lambda \int dt_1 \chi_{1L}(t_1) \sum_k \frac{1}{\sqrt{\omega_k L}} e^{i(\omega_k + \Omega)t_1} \sin\left(\frac{k\pi}{L}x_1\right) |e\rangle |g\rangle \hat{a}_k^\dagger |0\rangle + O(\lambda^2), \end{aligned} \quad (\text{B2})$$

where χ_{1L} -switching function for the first detector in the case that the right detector interacts before the left one, χ_{2L} -switching function for the second detector in the case that the right detector interacts earlier. In this case, we have that $\chi_{1L}(t) = 1$ for $t \in (0, T)$ and $\chi_{1L}(t) = 0$ for any other time. Similarly, $\chi_{2L}(t) = 1$ for $t \in (\Delta\tau, \Delta\tau + T)$ and $\chi_{2L}(t) = 0$ for any other time. It's worth noting that $\chi_{1L} = \chi_{2R}$ and $\chi_{2L} = \chi_{1R}$. After using this property describing relations between switching functions, we have

$$\begin{aligned} |\psi_R\rangle &= \hat{U}_1 \hat{U}_2 |g\rangle |g\rangle |0\rangle = |g\rangle |g\rangle |0\rangle - i\lambda \int dt_2 \chi_{2R}(t_2) \sum_k \frac{1}{\sqrt{\omega_k L}} e^{i(\omega_k + \Omega)t_2} \sin\left(\frac{k\pi}{L}x_2\right) |g\rangle |e\rangle \hat{a}_k^\dagger |0\rangle \\ &- i\lambda \int dt_1 \chi_{1R}(t_1) \sum_k \frac{1}{\sqrt{\omega_k L}} e^{i(\omega_k + \Omega)t_1} \sin\left(\frac{k\pi}{L}x_1\right) |e\rangle |g\rangle \hat{a}_k^\dagger |0\rangle + O(\lambda^2), \end{aligned} \quad (\text{B3})$$

$$\begin{aligned} |\psi_L\rangle &= \hat{U}_2 \hat{U}_1 |g\rangle |g\rangle |0\rangle = |g\rangle |g\rangle |0\rangle - i\lambda \int dt_2 \chi_{2R}(t_2) \sum_k \frac{1}{\sqrt{\omega_k L}} e^{i(\omega_k + \Omega)t_2} \sin\left(\frac{k\pi}{L}x_1\right) |e\rangle |g\rangle \hat{a}_k^\dagger |0\rangle \\ &- i\lambda \int dt_1 \chi_{1R}(t_1) \sum_k \frac{1}{\sqrt{\omega_k L}} e^{i(\omega_k + \Omega)t_1} \sin\left(\frac{k\pi}{L}x_2\right) |g\rangle |e\rangle \hat{a}_k^\dagger |0\rangle + O(\lambda^2). \end{aligned} \quad (\text{B4})$$

For simplicity of further calculation, let us introduce the following notation:

$$|\psi_R\rangle = \hat{U}_1 \hat{U}_2 |g\rangle |g\rangle |0\rangle = |gg\rangle |0\rangle + |ge\rangle |\phi_{ge}^R\rangle + |eg\rangle |\phi_{eg}^R\rangle + O(\lambda^2), \quad (\text{B5})$$

$$|\psi_L\rangle = \hat{U}_2 \hat{U}_1 |g\rangle |g\rangle |0\rangle = |gg\rangle |0\rangle + |ge\rangle |\phi_{ge}^L\rangle + |eg\rangle |\phi_{eg}^L\rangle + O(\lambda^2), \quad (\text{B6})$$

where $|\phi_{ge}^L\rangle$ —a state of a field when the left detector interacts first but the right detector is excited; $|\phi_{ge}^R\rangle$ —a state of a field when the left detector interacts first and the left detector is excited; $|\phi_{eg}^R\rangle$ —a state of a field when the right detector interacts first and the right detector is excited; and $|\phi_{eg}^L\rangle$ —a state of a field when the right detector interacts first but the left detector is excited as a consequence of the interaction between atoms and the field.

APPENDIX C: METHOD OF FINDING APPROPRIATE PARAMETERS

In this Appendix, we will find an appropriate set of parameters that orthogonalize $|\Phi_R\rangle$ and $|\Phi_L\rangle$ vectors,

$$\begin{aligned} |\Phi_R\rangle &= -i\lambda \sum_k \frac{1}{\sqrt{\omega_k L}} \int dt \left(\chi_{2R}(t) \sin\left(\frac{k\pi}{L}x_2\right) + \chi_{1R}(t) \sin\left(\frac{k\pi}{L}x_1\right) \right) e^{i(\omega_k + \Omega)t} \hat{a}_k^\dagger |0\rangle \\ &= -i\lambda \sum_k \int dt (\chi_{2R}(t) u_k(x_2) + \chi_{1R}(t) u_k(x_1)) e^{i(\omega_k + \Omega)t} \hat{a}_k^\dagger |0\rangle \\ &= -\lambda \sum_k \frac{e^{iT(\omega_k + \Omega)} - 1}{\omega_k + \Omega} (e^{i\Delta\tau(\omega_k + \Omega)} u_k(x_1) + u_k(x_2)) \hat{a}_k^\dagger |0\rangle \end{aligned} \quad (\text{C1})$$

$$\begin{aligned} |\Phi_L\rangle &= -i\lambda \sum_k \frac{1}{\sqrt{\omega_k L}} \int dt \left(\chi_{2R}(t) \sin\left(\frac{k\pi}{L}x_1\right) + \chi_{1R}(t) \sin\left(\frac{k\pi}{L}x_2\right) \right) e^{i(\omega_k + \Omega)t} \hat{a}_k^\dagger |0\rangle \\ &= -\lambda \sum_k \frac{e^{iT(\omega_k + \Omega)} - 1}{\omega_k + \Omega} (e^{i\Delta\tau(\omega_k + \Omega)} u_k(x_2) + u_k(x_1)) \hat{a}_k^\dagger |0\rangle, \end{aligned} \quad (\text{C2})$$

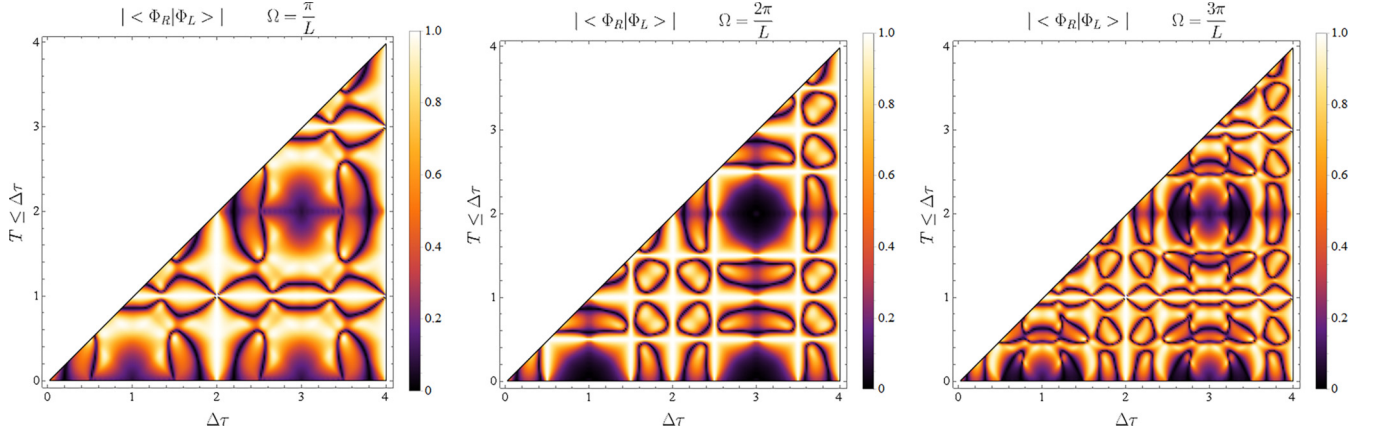


FIG. 7. The analysis of an orthogonality between $|\Phi_L\rangle$ and $|\Phi_R\rangle$ for different parameters describing interaction. An absolute value of the scalar product for two detectors standing at $x_1 = L/4$ and $x_2 = 3L/4$. The energy gap Ω is chosen as one of the cavity frequencies. Scalar product approximated as a finite sum of 30 modes, i.e., $N_k = N_n = 30$.

where the form of the state $|\Phi_L\rangle$ we get by changing $x_1 \longleftrightarrow x_2$. Now it is easy to see that the scalar product can be written as

$$\begin{aligned} \langle \Phi_R | \Phi_L \rangle &\cong \lambda^2 \sum_k \frac{|e^{iT(\omega_k + \Omega)} - 1|^2}{(\omega_k + \Omega)^2} (e^{-i\Delta\tau(\omega_k + \Omega)} u_k(x_1) + u_k(x_2)) (e^{i\Delta\tau(\omega_k + \Omega)} u_k(x_2) + u_k(x_1)) \\ &\cong 2\lambda^2 \sum_k \frac{e^{-i\Delta\tau(\omega_k + \Omega)}}{(\omega_k + \Omega)^2} [1 - \cos(T(\omega_k + \Omega))] (u_k(x_1) + e^{i\Delta\tau(\omega_k + \Omega)} u_k(x_2))^2. \end{aligned} \quad (C3)$$

We have to remember that states $|\Phi_L\rangle$ and $|\Phi_R\rangle$ were not properly normalized, so now we can find the norm:

$$\begin{aligned} \|\Phi_R\| &= \sqrt{\langle \Phi_R | \Phi_R \rangle} = \sqrt{\lambda^2 \sum_k \frac{|e^{iT(\omega_k + \Omega)} - 1|^2}{(\omega_k + \Omega)^2} |e^{i\Delta\tau(\omega_k + \Omega)} u_k(x_1) + u_k(x_2)|^2} \\ &= 2\lambda \sqrt{\sum_k \frac{\sin^2 \frac{T(\omega_k + \Omega)}{2}}{(\omega_k + \Omega)^2} [u_k(x_1)^2 + 2u_k(x_1)u_k(x_2) \cos(\Delta\tau(\omega_k + \Omega)) + u_k(x_2)^2]} \end{aligned} \quad (C4)$$

$$\|\Phi_L\| = \sqrt{\langle \Phi_L | \Phi_L \rangle} = 2\lambda \sqrt{\sum_k \frac{\sin^2 \frac{T(\omega_k + \Omega)}{2}}{(\omega_k + \Omega)^2} [u_k(x_2)^2 + 2u_k(x_2)u_k(x_1) \cos(\Delta\tau(\omega_k + \Omega)) + u_k(x_1)^2]}. \quad (C5)$$

We can notice that $\|\Phi_R\| = \|\Phi_L\|$ and, finally, the scalar product has the following form:

$$\langle \Phi_R | \Phi_L \rangle = \frac{\langle \Phi_R | \Phi_L \rangle}{\|\Phi_R\| \|\Phi_L\|} = \frac{\sum_k \frac{e^{-i\Delta\tau(\omega_k + \Omega)}}{(\omega_k + \Omega)^2} [1 - \cos(T(\omega_k + \Omega))] (u_k(x_1) + e^{i\Delta\tau(\omega_k + \Omega)} u_k(x_2))^2}{2 \sum_n \frac{\sin^2 \frac{T(\omega_n + \Omega)}{2}}{(\omega_n + \Omega)^2} [u_n(x_2)^2 + 2u_n(x_2)u_n(x_1) \cos(\Delta\tau(\omega_n + \Omega)) + u_n(x_1)^2]}. \quad (C6)$$

This function can be estimated as a finite sum. Let us denote the upper limits of these two sums as N_n for the sum over n and N_k for the sum over k .

Figure 6 shows the absolute value of the scalar product as a function of the energy gap Ω plotted for different numbers of modes N_n and N_k . We can see that we can produce entanglement for very short times $\Delta\tau = T = L/10$. Thus, it proves that there is also an entanglement between two cavities for spacelike separated events of interaction.

Figure 6 looks quite random. Let us analyze the scalar product for the case of two detectors standing in the positions $x_1 = L/4$ and $x_2 = 3L/4$. Figure 7 shows the absolute value of the scalar product for different parameters $\Delta\tau$ and $T \leq \Delta\tau$ for different values of the energy gap Ω . We can notice that there are many parameters minimizing the scalar product between two states.

Based on Fig. 7, we can conjecture that point $(\Delta\tau, T) = (3L, 2L)$ is a good candidate for the orthogonalization of the states $|\Phi_R\rangle$ and $|\Phi_L\rangle$. To verify this hypothesis, let us consider the following calculation: Let $L = 1$, $x_1 = 1/4$, $x_2 = 3/4$, $\Omega = \pi$, $\Delta\tau = 3$, $T = 2 + \epsilon$, where $\epsilon \in \mathbb{R}_+$ is a small parameter. Then

$$\langle \Phi_R | \Phi_L \rangle = - \frac{\sum_k \frac{e^{-3ik\pi}}{k(k+1)^2} [\cos((1+k)(2+\epsilon)\pi) - 1] (\sin \frac{k\pi}{4} - e^{3ik\pi} \sin \frac{3k\pi}{4})^2}{2 \sum_n \frac{\sin^2 \frac{(n+1)\pi\epsilon}{2}}{2n(n+1)^2} [(1+2(-1)^n) \cos \frac{n\pi}{2} + \cos \frac{3n\pi}{2} - 4]}. \quad (C7)$$

Each of these sums can be done analytically for arbitrary ϵ . Then we expand the numerator and denominator around $\epsilon = 0$ to get

$$|\langle \Phi_R | \Phi_L \rangle| = \left| \frac{\frac{1}{2\pi}(2 \ln 20 \ln(1-i) - \ln(1+i))\epsilon^2 + O(\epsilon^3)}{\frac{1}{6\pi}(9 + \ln 8 - 6 \ln \pi - 6 \ln \epsilon)\epsilon^2 + O(\epsilon^3)} \right| \approx \frac{\ln 8}{9 + \ln 8 - 6 \ln \pi \epsilon}. \quad (\text{C8})$$

And we see that

$$\lim_{\epsilon \rightarrow 0^+} |\langle \Phi_R | \Phi_L \rangle| = 0. \quad (\text{C9})$$

APPENDIX D: SECOND ORDER OF THE DYSON SERIES

In this Appendix, we will show that second-order Dyson expansion does not affect $|\Phi_R\rangle$ and $|\Phi_L\rangle$.

One can ask the question why (C3) depends on λ^2 . Previously, we limited our calculation only to the first-order expansion of the Dyson series. We have to verify that second-order expansion does not produce lambda square terms too. Otherwise, there is a possibility that results from (C3) will cancel out with these additional terms. Let us write the general evolution operator in the following form:

$$\begin{aligned} \hat{U} = & \mathbb{1} - i\lambda \int_{-\infty}^{\infty} dt \chi_d(t) (e^{i\Omega t} \hat{\sigma}^+ + e^{-i\Omega t} \hat{\sigma}^-) \sum_n (\hat{a}_n^\dagger u_n(x_d) e^{i\omega_n t} + \hat{a}_n u_n(x_d) e^{-i\omega_n t}) \\ & - \lambda^2 \int_{-\infty}^{\infty} dt_2 \int_{-\infty}^{t_2} dt_1 \chi_d(t_2) \chi_d(t_1) (e^{i\Omega t_2} \hat{\sigma}^+ + e^{-i\Omega t_2} \hat{\sigma}^-) (e^{i\Omega t_1} \hat{\sigma}^+ + e^{-i\Omega t_1} \hat{\sigma}^-) \\ & \times \sum_n (\hat{a}_n^\dagger u_n(x_d) e^{i\omega_n t_2} + \hat{a}_n u_n(x_d) e^{-i\omega_n t_2}) \sum_m (\hat{a}_m^\dagger u_m(x_d) e^{i\omega_m t_1} + \hat{a}_m u_m(x_d) e^{-i\omega_m t_1}), \end{aligned} \quad (\text{D1})$$

where x_d is a position of a detector and $\hat{\sigma}^\pm$ acts on the internal state of this detector. In our case, we have two detectors and two Hilbert spaces of internal DoFs. We can simplify the notation to write operators of the evolution as

$$\hat{U}_1 = \mathbb{1} - i\lambda \sum_n (\hat{U}_{1n}^+ \hat{\sigma}_1^+ + \hat{U}_{1n}^- \hat{\sigma}_1^-) - \lambda^2 \sum_{n,m} (\hat{U}_{1nm}^{++} \hat{\sigma}_1^+ \hat{\sigma}_1^+ + \hat{U}_{1nm}^{+-} \hat{\sigma}_1^+ \hat{\sigma}_1^- + \hat{U}_{1nm}^{-+} \hat{\sigma}_1^- \hat{\sigma}_1^+ + \hat{U}_{1nm}^{--} \hat{\sigma}_1^- \hat{\sigma}_1^-), \quad (\text{D2})$$

$$\hat{U}_2 = \mathbb{1} - i\lambda \sum_n (\hat{U}_{2n}^+ \hat{\sigma}_2^+ + \hat{U}_{2n}^- \hat{\sigma}_2^-) - \lambda^2 \sum_{n,m} (\hat{U}_{2nm}^{++} \hat{\sigma}_2^+ \hat{\sigma}_2^+ + \hat{U}_{2nm}^{+-} \hat{\sigma}_2^+ \hat{\sigma}_2^- + \hat{U}_{2nm}^{-+} \hat{\sigma}_2^- \hat{\sigma}_2^+ + \hat{U}_{2nm}^{--} \hat{\sigma}_2^- \hat{\sigma}_2^-), \quad (\text{D3})$$

where U_{1n}^\pm, U_{2n}^\pm are operators from the first-order order expansion and $U_{1nm}^{\pm\pm}$ and $U_{2nm}^{\pm\pm}$ are operators from the second-order expansion of the Dyson series. $\hat{\sigma}_1^\pm$ and $\hat{\sigma}_2^\pm$ are operators $\hat{\sigma}^\pm$ acting on the internal space of the first or second detector, respectively. To find contributions proportional to the λ^2 to the value of (C3), we have to find new terms in the $|\psi_R\rangle$ and $|\psi_L\rangle$ proportional to $|ge\rangle$ or $|eg\rangle$. Knowing that $|\psi_R\rangle = \hat{U}_1 \hat{U}_2 |gg\rangle|0\rangle$, $|\psi_L\rangle = \hat{U}_2 \hat{U}_1 |gg\rangle|0\rangle$, $\hat{\sigma}^- |g\rangle = 0$ and $\hat{\sigma}^+ |e\rangle = 0$ we can write

$$|\psi_R\rangle = \left[\mathbb{1} - i\lambda \sum_n \hat{U}_{1n}^+ \hat{\sigma}_1^+ - \lambda^2 \sum_{n,m} \hat{U}_{1nm}^{-+} \hat{\sigma}_1^- \hat{\sigma}_1^+ \right] \left[\mathbb{1} - i\lambda \sum_n \hat{U}_{2n}^+ \hat{\sigma}_2^+ - \lambda^2 \sum_{n,m} \hat{U}_{2nm}^{-+} \hat{\sigma}_2^- \hat{\sigma}_2^+ \right] |gg\rangle|0\rangle, \quad (\text{D4})$$

$$|\psi_L\rangle = \left[\mathbb{1} - i\lambda \sum_n \hat{U}_{2n}^+ \hat{\sigma}_2^+ - \lambda^2 \sum_{n,m} \hat{U}_{2nm}^{-+} \hat{\sigma}_2^- \hat{\sigma}_2^+ \right] \left[\mathbb{1} - i\lambda \sum_n \hat{U}_{1n}^+ \hat{\sigma}_1^+ - \lambda^2 \sum_{n,m} \hat{U}_{1nm}^{-+} \hat{\sigma}_1^- \hat{\sigma}_1^+ \right] |gg\rangle|0\rangle. \quad (\text{D5})$$

We can observe that second-order contributions from the same detector do not change the internal state, i.e., $\hat{\sigma}^- \hat{\sigma}^+ |g\rangle = |g\rangle$, while the product of first-order terms from both detectors gives $\hat{\sigma}_1^+ \hat{\sigma}_2^+ |gg\rangle = \hat{\sigma}_2^+ \hat{\sigma}_1^+ |gg\rangle = |ee\rangle$. Thus, the second-order terms do not have support on the subspace spanned by states $|ge\rangle, |eg\rangle$. Note that states $|ge\rangle$ or $|eg\rangle$ appear in this expansion at order λ^3 or higher. This means that second-order terms from the Dyson series do not affect states $|\Phi_R\rangle$ and $|\Phi_L\rangle$ in our approximation.

- [1] J. Butterfield and C. Isham, Spacetime and the philosophical challenge of quantum gravity, in *Physics Meets Philosophy at the Planck Scale*, edited by C. Callender and N. Huggett (Cambridge University Press, Cambridge, United Kingdom, 2001), p. 33.
- [2] L. Hardy, Towards quantum gravity: A framework for probabilistic theories with non-fixed causal structure, *J. Phys. A: Math. Theor.* **40**, 3081 (2007).

- [3] G. Chiribella, G. M. D'Ariano, P. Perinotti, and B. Valiron, Quantum computations without definite causal structure, *Phys. Rev. A* **88**, 022318 (2013).
- [4] *Approaches to Quantum Gravity: Toward a New Understanding of Space, Time and Matter*, edited by D. Oriti (Cambridge University Press, Cambridge, United Kingdom, 2009).
- [5] C. Kiefer, *Quantum Gravity*, 3rd ed., International Series of Monographs on Physics (OUP, Oxford, 2012).

- [6] M. Zych, F. Costa, I. Pikovski, and Čslav Brukner, Bell's theorem for temporal order, *Nat. Commun.* **10**, 1 (2019).
- [7] A. Dimić, M. Milivojević, D. Gočanin, N. S. Móller, and Čslav Brukner, Simulating indefinite causal order with Rindler observers, *Front. Phys.* **8**, 470 (2020).
- [8] L. M. Procopio, A. Moqanaki, M. Araújo, F. Costa, I. A. Calafell, E. G. Dowd, D. R. Hamel, L. A. Rozema, Č. Brukner, and P. Walther, Experimental superposition of orders of quantum gates, *Nat. Commun.* **6**, 7913 (2015).
- [9] G. Rubino, L. A. Rozema, A. Feix, M. Araújo, J. M. Zeuner, L. M. Procopio, Č. Brukner, and P. Walther, Experimental verification of an indefinite causal order, *Sci. Adv.* **3**, 1602589 (2017).
- [10] G. Rubino, L. A. Rozema, F. Massa, M. Araújo, M. Zych, Č. Brukner, and P. Walther, Experimental entanglement of temporal orders, *Quantum* **6**, 621 (2022).
- [11] K. Goswami, C. Giarmatzi, M. Kewming, F. Costa, C. Branciard, J. Romero, and A. G. White, Indefinite causal order in a quantum switch, *Phys. Rev. Lett.* **121**, 090503 (2018).
- [12] Y. Guo, X.-M. Hu, Z.-B. Hou, H. Cao, J.-M. Cui, B.-H. Liu, Y.-F. Huang, C.-F. Li, G.-C. Guo, and G. Chiribella, Experimental investigating communication in a superposition of causal orders, *Phys. Rev. Lett.* **124**, 030502 (2020).
- [13] K. Wei, N. Tischler, S.-R. Zhao, Y.-H. Li, J. M. Arrazola, Y. Liu, W. Zhang, H. Li, L. You, Z. Wang, Y.-A. Chen, B. C. Sanders, Q. Zhang, G. J. Pryde, F. Xu, and J.-W. Pan, Experimental quantum switching for exponentially superior quantum communication complexity, *Phys. Rev. Lett.* **122**, 120504 (2019).
- [14] M. M. Taddei, J. Cariñe, D. Martínez, T. García, N. Guerrero, A. A. Abbott, M. Araújo, C. Branciard, E. S. Gómez, S. P. Walborn, L. Aolita, and G. Lima, Computational advantage from the quantum superposition of multiple temporal orders of photonic gates, *PRX Quantum* **2**, 010320 (2021).
- [15] S. Bose, A. Mazumdar, G. W. Morley, H. Ulbricht, M. Toroš, M. Paternostro, A. Geraci, P. Barker, M. S. Kim, and G. Milburn, Spin entanglement witness for quantum gravity, *Phys. Rev. Lett.* **119**, 240401 (2017).
- [16] C. Marletto and V. Vedral, Gravitationally induced entanglement between two massive particles is sufficient evidence of quantum effects in gravity, *Phys. Rev. Lett.* **119**, 240402 (2017).
- [17] M. Zych, F. Costa, I. Pikovski, and Č. Brukner, Quantum interferometric visibility as a witness of general relativistic proper time, *Nat. Commun.* **2**, 505 (2011).
- [18] I. Pikovski, M. Zych, F. Costa, and C. Brukner, Time dilation in quantum systems and decoherence, *New J. Phys.* **19**, 025011 (2017).
- [19] Y. Margalit, O. Dobkowski, Z. Zhou, O. Amit, Y. Japha, S. Moukouri, D. Rohrlich, A. Mazumdar, S. Bose, C. Henkel, and R. Folman, Realization of a complete Stern-Gerlach interferometer: Toward a test of quantum gravity, *Sci. Adv.* **7** (2021).
- [20] B. Yurke and D. Stoler, Bell's-inequality experiments using independent-particle sources, *Phys. Rev. A* **46**, 2229 (1992).
- [21] A. Dragan, *Unusually Special Relativity* (World Scientific, London, 2021).
- [22] M. Araújo, C. Branciard, F. Costa, A. Feix, C. Giarmatzi, and Č. Brukner, Witnessing causal nonseparability, *New J. Phys.* **17**, 102001 (2015).
- [23] C. Branciard, Witnesses of causal nonseparability: An introduction and a few case studies, *Sci. Rep.* **6**, 26018 (2016).
- [24] W. G. Unruh, Notes on black-hole evaporation, *Phys. Rev. D* **14**, 870 (1976).
- [25] W. G. Unruh and R. M. Wald, What happens when an accelerating observer detects a rindler particle, *Phys. Rev. D* **29**, 1047 (1984).
- [26] L. C. B. Crispino, A. Higuchi, and G. E. Matsas, The unruh effect and its applications, *Rev. Mod. Phys.* **80**, 787 (2008).